Coupled Nonlinear Microwave Oscillators

Jonathan Dixon
May 10, 1994

Abstract

In this paper, I explore the nonlinear characteristics of microwave FET oscillators through the use of mathematical modeling. The FET is reduced to non-linear circuit elements through the use of the Curtice Cubic model; linear circuit elements are used to model bias lines and the output antenna. The circuit elements are reduced to a set of coupled nonlinear ordinary differential equations through the use of Kirchhoff's current law. The circuit is first tested in isolation, then it is driven by a fixed oscillator. Finally, two oscillators are coupled together through their antennas. One set of results in the fixed oscillator simulations strongly suggests that chaotic behavior is present in the system.

I. Introduction

There are a wide variety of sources used today in microwave systems. The choice of source to use for a particular system is generally based on the intended application for that system. Traditionally, low power systems have used solid-state sources such as Gunn diodes, IMPATT (IMPact Avalanche Transit Time) diodes, and transistor oscillators, while high-power systems have used tube-based designs, such as magnetrons, klystrons, and traveling wave tubes [1].

Recently, however, people have investigated making high-power sources using field-effect transistors (FETs), which could be integrated into circuits such as monolithic microwave integrated circuits (MMICs). This would allow easier production and increased reliability since everything could be done with solid-state circuitry. Since the power levels desired were beyond the capability of single FETs, it became necessary to combine the outputs of many oscillator circuits simultaneously. Initially this was done with passive feed networks, but these networks became very complicated and were generally lossy.

Because of these difficulties, other means of combining the outputs of these FET oscillators were desired. Recently, much interest has been focused on the use of planar grids of oscillators which combine the power from many oscillators quasi-optically [2]. These grids couple a large number of oscillators together to provide the desired output power. This combining occurs in free space, so the losses due to the complex feed networks are eliminated. In order to get maximum power, high spectral purity, and an optimal antenna pattern (narrow main lobe and low side lobes) from the grid, it is necessary to get the oscillators to have identical phases as well as frequencies. This is often achieved through the use of back mirrors or complete Fabry-Perot cavities. Both of these set up a cavity mode structure which facilitates locking at the desired frequency.

Because the FETs are driven in the large-signal regime, they are highly nonlinear, which results in the oscillator circuits being nonlinear as well. It has been seen ([3]-[7]) that nonlinear oscillators often behave in a chaotic manner, which can dramatically affect the locking characteristics of the oscillators. In many cases, this behavior causes small variations in system parameters to effect large fluctuations in the amount of coupling needed to get two oscillators to lock. Since little is known about the dynamics of the locking of large grids, it is therefore desirable to examine the effects of parametric variations on the locking characteristics of microwave oscillators, paying special attention to results which suggest chaotic behavior in the system.

II. Nonlinear FET Models

There have been a number of different models developed to account for the nonlinear behavior of microwave MESFETs (Metal-Semiconductor FETs). A widely used microwave circuit simulation tool, for example, provides a choice of five different FET models: Curtice Quadratic, Curtice Cubic, Statz, Materka, and Tajima [8]. Two of these models, the Curtice Quadratic and the Curtice Cubic, are based on a general model developed by Curtice and Ettenberg [9] which models the drain-source current with a hyperbolic tangent multiplied by a fitting polynomial of a given order (e.g., third order for the Curtice Cubic).

For the cubic model, we have:

$$I_{ds} = \left(a_0 + a_1 v_1 + a_2 v_1^2 + a_3 v_1^3 \right) \tanh\left(\gamma v_{ds}\right) , \tag{1}$$

where $v_1 = v_{gs} \left[1 + \beta \left(v_{ds0} - v_{ds} \right) \right]$.

The model also includes parasitic capacitances and inductances. The parasitics C_{gs} and C_{gd} are nonlinear capacitances caused by reverse-biased diodes, and their values are given by the equation

$$C_{gs,\,gd} = C_{gs0,\,gd0} \left(1 - \frac{V_{applied}}{V_{bi}} \right)^{-1/2} . \tag{2}$$

The Curtice Cubic model has found widespread acceptance, and the equations needed are not too computationally complex, so I chose to use it for the purpose of my simulations. The full circuit model is shown in Figure 1.

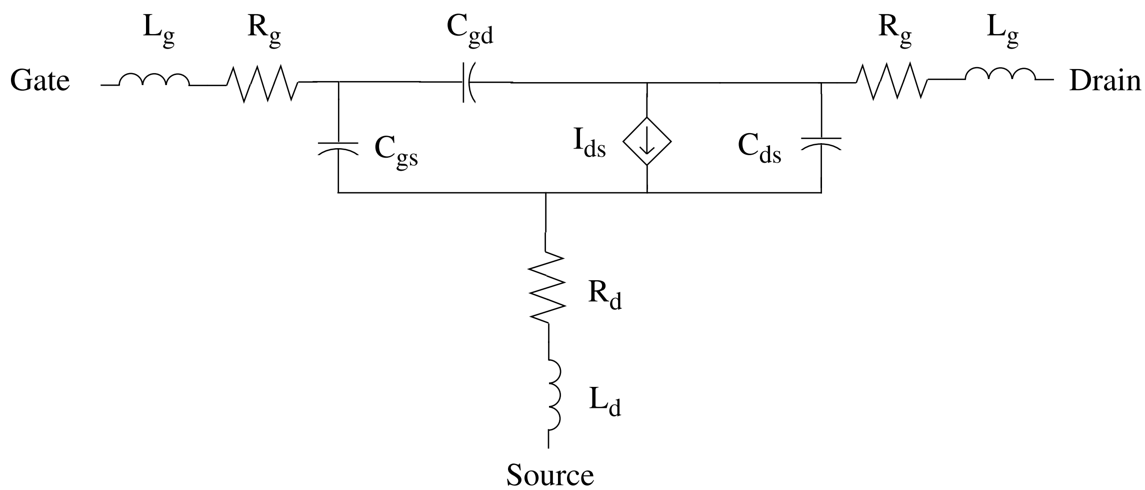

Figure 1. Curtice-Ettenberg FET model

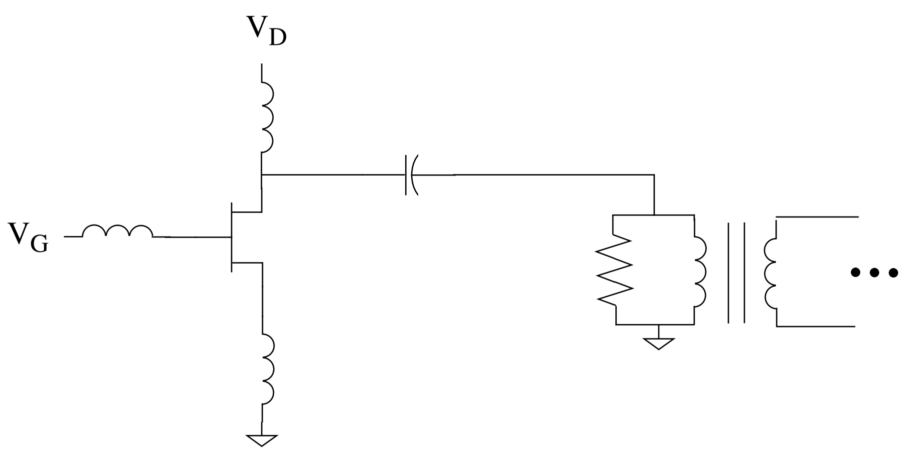

Figure 2. Common-source FET oscillator

III. Microwave FET Oscillator Circuits

There are several different types of FET oscillators commonly used at microwave frequencies. Most, however, are extensions of either the common-source or common-gate configuration, so those were the topologies I considered for my simulations.

I initially looked at an oscillator circuit using the common-source configuration (Figure 2, circuit is mirrored around the mutual inductance as represented by the dots) because this was the arrangement I have the most experience using. It uses inductors on all three ports of the FET to allow biasing of the device (source through an inductor to ground, gate through inductor to V_G, and drain through inductor to V_D) while uncoupling that biasing from the AC signal. The output of the oscillator is taken from the drain through a capacitor to a resistor in parallel with a mutual

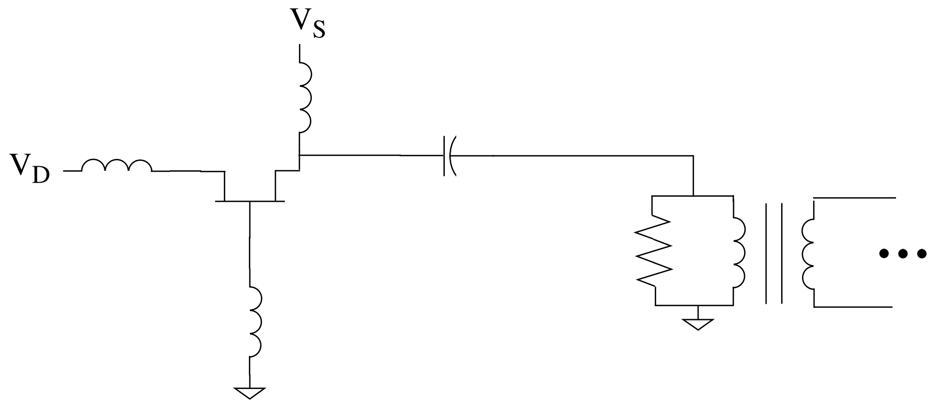

Figure 3. Common-gate FET oscillator

inductance, which represents the load impedance and coupling of an antenna. The antenna allows the output power to be coupled into free-space as well as provides the coupling between the oscillators. A similar design is used by Martinez and Compton [10], which also uses a similar model for the coupling of two antennas. This design does not work well for the transistor parameters I was using. The drain inductor and coupling capacitor tend to dominate the response of the circuit, rather than the source inductance and drain-source capacitance as is generally seen in actual circuits.

I then changed to a common-gate circuit (Figure 3), similar to that used by Liao and York [11]. This configuration is significantly more unstable due to the increased feedback provided by I_{ds} and C_{ds} instead of just C_{gd}, which is generally quite small. This makes it more likely to make a good oscillator. The gate is connected through an inductor to ground, and the drain and source are connected to their respective voltages through inductors. The antenna is represented by the same subcircuit as in the common-source configuration, but is connected to the source instead. This arrangement produces sustained oscillations which were primarily determined by the gate inductance and the gate-source capacitance as expected. That is why I chose to use this design for the remainder of this work.

IV. Mathematical Modeling

Once the circuit topology was decided upon, a reduced version of the Curtice Cubic model was inserted in the circuit in place of the FET, as shown in Figure 4. In order to reduce the number of differential equations needed to represent the circuit, the parasitic resistance and inductance of

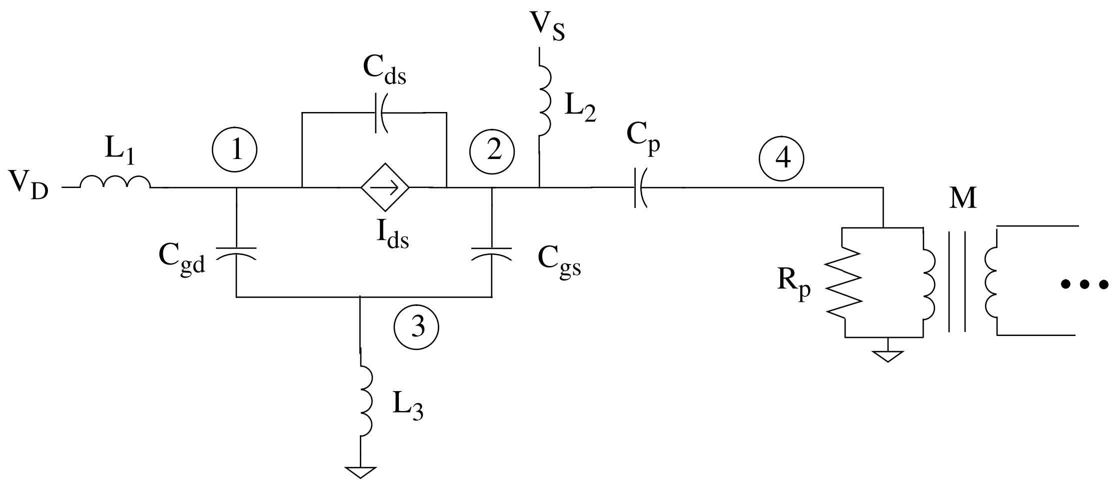

Figure 4. Complete oscillator circuit

the leads has been ignored, with the assumption that they are not significant compared to the external elements attached to the device. Since the design of FETs is usually optimized to reduce these parasitics, this is generally a good assumption below about 50 GHz.

Kirchhoff's current law was then used to write four node equations. Initially, the voltages of the four nodes were used as the independent variables, but it was found that with this arrangement of capacitors these voltages did not form a suitable basis function for the circuit, which caused the resulting system of equations to be singular. A basis constructed of the differences between the node voltages was found to be more desirable mathematically, resulting in the bases $u_1 = v_1 - v_3$, $u_2 = v_2 - v_3$, $u_3 = v_2 - v_4$, and $u_4 = v_4$ being chosen.

This resulted in a set of four node equations:

$$\frac{1}{L_1}\int (u_1 - u_2 + u_3 + u_4 - v_D)\, dt + C_{gd}\dot{u}_1 + I_{ds} + C_{gs}(\dot{u}_1 - \dot{u}_2) = 0\,, \qquad (3a)$$

$$-I_{ds} + C_{ds}\left(\dot{u}_2 - \dot{u}_1\right) + C_{gs}\dot{u}_2 + C_p\dot{u}_3 + \frac{1}{L_2}\int (u_3 + u_4 - v_S)\, dt = 0\,, \qquad (3b)$$

$$-C_{gs}\dot{u}_2 - C_{gd}\dot{u}_1 + \frac{1}{L_3}\int (-u_2 + u_3 + u_4)\, dt = 0\,, \qquad (3c)$$

and

$$C_p\dot{u}_3 = \frac{u_4}{R_p} + M\int \hat{u}_4 dt\,. \qquad (3d)$$

The variable $\hat{u}_4$ which appears in (3d) is the voltage from the companion oscillator which drives the mutual inductance, and the dots over variables represent derivatives with respect to time. I_{ds} is as given in (1) and C_{gs} and C_{gd} are as given in (2).

Differentiating (3a)-(3d) once to remove the integrals gives three second-order ordinary differential equations and one first-order ordinary differential equation. By introducing three new variables, $u_5 = \dot{u}_1$, $u_6 = \dot{u}_2$, and $u_1 = \dot{u}_3$, and applying some algebra, these equations can be reduced to seven first-order nonlinear coupled ordinary differential equations:

$$\dot{u}_1 = u_5, \tag{4a}$$

$$\dot{u}_2 = u_6, \tag{4b}$$

$$\dot{u}_3 = u_7, \tag{4c}$$

$$\dot{u}_4 = R_p\left(C\dot{u}_7 - M\hat{u}_4 \right), \tag{4d}$$

$$\dot{u}_5 = \frac{h + g\,(C_{ds}/C_{gs})}{C_{ds} + C_{gd} + C_{gd}\,(C_{ds}/C_{gs})}, \tag{4e}$$

$$\dot{u}_6 = \frac{g - C_{gd}\dot{u}_5}{C_{gs}}, \tag{4f}$$

and

$$\dot{u}_7 = \frac{\dot{I}_{ds} + C_{ds}\,(\dot{u}_5 - \dot{u}_6) - C_{gs}\dot{u}_6 - \dot{C}_{gs}u_6 + \dfrac{(-u_3 - u_4 + v_S)}{L_2}}{C_p}, \tag{4g}$$

where

$$g = \frac{-u_2 + u_3 + u_4}{L_3} - \dot{C}_{gs}u_6 - \dot{C}_{gd}u_5$$

and

$$h = \frac{-u_1 + u_3 - u_3 - u_4 + v_D}{L_1} - \dot{C}_{gd}u_5 - \dot{I}_{ds}.$$

Equations (4a)-(4g) are solved numerically using fourth-order Runge-Kutta, using about 300 time-steps per oscillation period. In calculating the derivatives, it is necessary to calculate the one for u_5 first, followed by the u_6 term, then the u_7 term, and finally the u_4 term, since each of these depends upon the terms calculated before it. Additional oscillators are added to the system by repeating this set of equations for each one desired and choosing the coupling as appropriate.

V. Free-running Single Oscillator

I began my work by looking at a single oscillator, to test the model of the circuit and find a combination of parameters which would give a sustained oscillation between 1 and 5 GHz. The transistor parameters used were polynomial coefficients of 1.8, 0.6712, –0.584, and -0.2346 (a_0 through a_3), γ of 2.0, v_{bi} of 0.8, β of 0.05, and v_{ds0} of 8.0. The transistor source was biased at 5.0 V, and the drain was at -0.1V. I found that using the circuit parameters of a 50 Ω antenna impedance (R_p), a 10 nF coupling capacitance (C_p), L_1 = 29 nH, L_2 = 19 nH, L_3 = 12 nH,

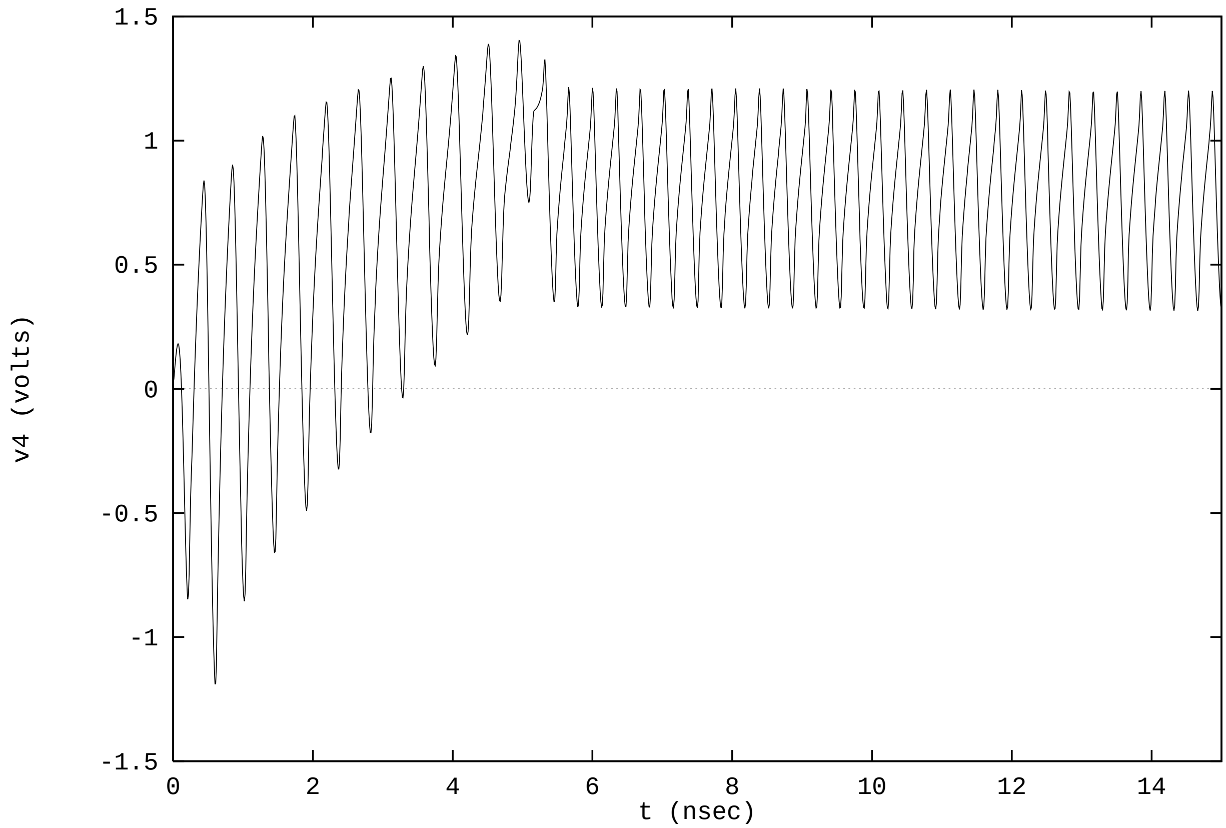

Figure 5. Free-running single oscillator

$C_{ds} = 0.1$ pF, $C_{gs0} = 0.6$ pF, and $C_{gd0} = 30$ fF gave an oscillation at 2.9 GHz, as shown in Figure 5.

The start-up transient for the oscillator takes about 6 ns, after which time the frequency and amplitude become quite stable. I believe that the abruptness of the change-over is due to the voltage across one or both of the nonlinear capacitors approaching v_{bi}, which would cause the capacitance to become large as the diode approached turn-on, and this would bound the obtainable voltages across those junctions. As long as L_1 and L_2 are kept higher than L_3, the frequency is primarily determined by L_3, as would be expected.

VI. Periodically Driven Single Oscillator

Next I drove the oscillator by coupling in a steady sine wave, similar to what would be obtained if one drove an oscillator with a master reference signal, as might be seen in a master-slave system. It is also similar to the set-up of an injection-locked oscillator. I investigated the ability of the oscillator to lock at a variety of levels of coupling at different frequencies near it's natural frequency.

In order to determine whether the oscillator had locked to the driving frequency, I took a

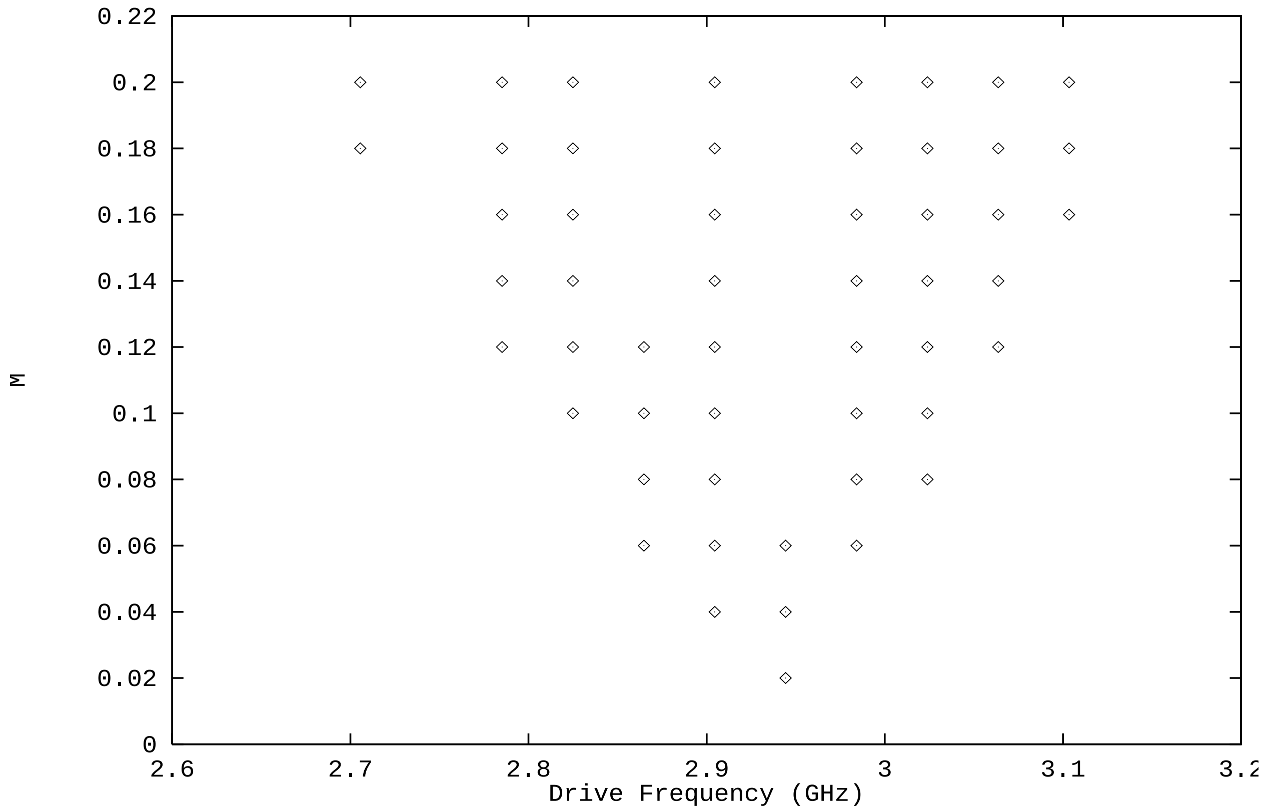

Figure 6. Locking ranges

Poincaré section of u_4 at the times when the drive crossed 0 in a positive direction. I then compared the change in the location of the sectioned point over a period of time, after allowing sufficient time for the transients to settle out. If the sum over a 25 ns period of the RMS error between the value of the present sectioned point and the previous three points was below 0.15, the oscillator was considered to be locked; otherwise it had failed to lock. The ability of the oscillator to lock was examined over a range of drive frequencies and coupling coefficients, and the results obtained are shown in Figure 6. In this figure, the symbols mark those pairs of coupling coefficients and drive frequencies where locking occurred. Even with the fairly rough scale, one can begin to see a structure similar in many ways to the finger structures previously seen in similar works ([6], for example).

An interesting result was obtained at a bit lower frequency, with $L_1 = L_2 = L_3 = 90$ nH, $C_{ds} = 5$ pF, $C_{gs0} = 12$ pF, and $C_{gd0} = 0.3$ pF. The natural frequency of the oscillator was 250 MHz, and the circuit was driven at a frequency of about 220 MHz with coupling of 0.05. As can be seen in Figure 7, this resulted in a 6-cycle (with gradually decaying DC component causing the paths not to quite line up). As discussed by Ott [12], a consequence of Šarkovskii's theorem is that the existence of this 6-cycle implies that the system has an infinite number of periodic orbits; in this case the implication is that all orbits with an even periodicity must exist in this system.

Even more interestingly, Li and Yorke [13] showed that for maps of an interval onto itself (or onto the set of real numbers as suggested in their closing remark), the existence of a 3-cycle implies the existence of chaos in a system. The mathematical model of this oscillator is quite similar to a map transforming an 8-dimensional interval of voltages and their derivatives onto that same interval at each timestep. Furthermore, it is quite likely that the 6-cycle that is seen here is the result of a bifurcation of a period three limit cycle which was not actually observed but would be adjacent in the parameter space. Therefore, it is reasonable to conditionally apply the conclusion of Li and Yorke, which means that the 6-cycle which is seen in the driven oscillator at least strongly suggests the presence of chaos in the system.

VII. Coupled Oscillator Pair

The next step was to combine two oscillators, allowing them to drive each other to investigate their locking properties. Unfortunately, in doing this I ran into a problem with my model. The

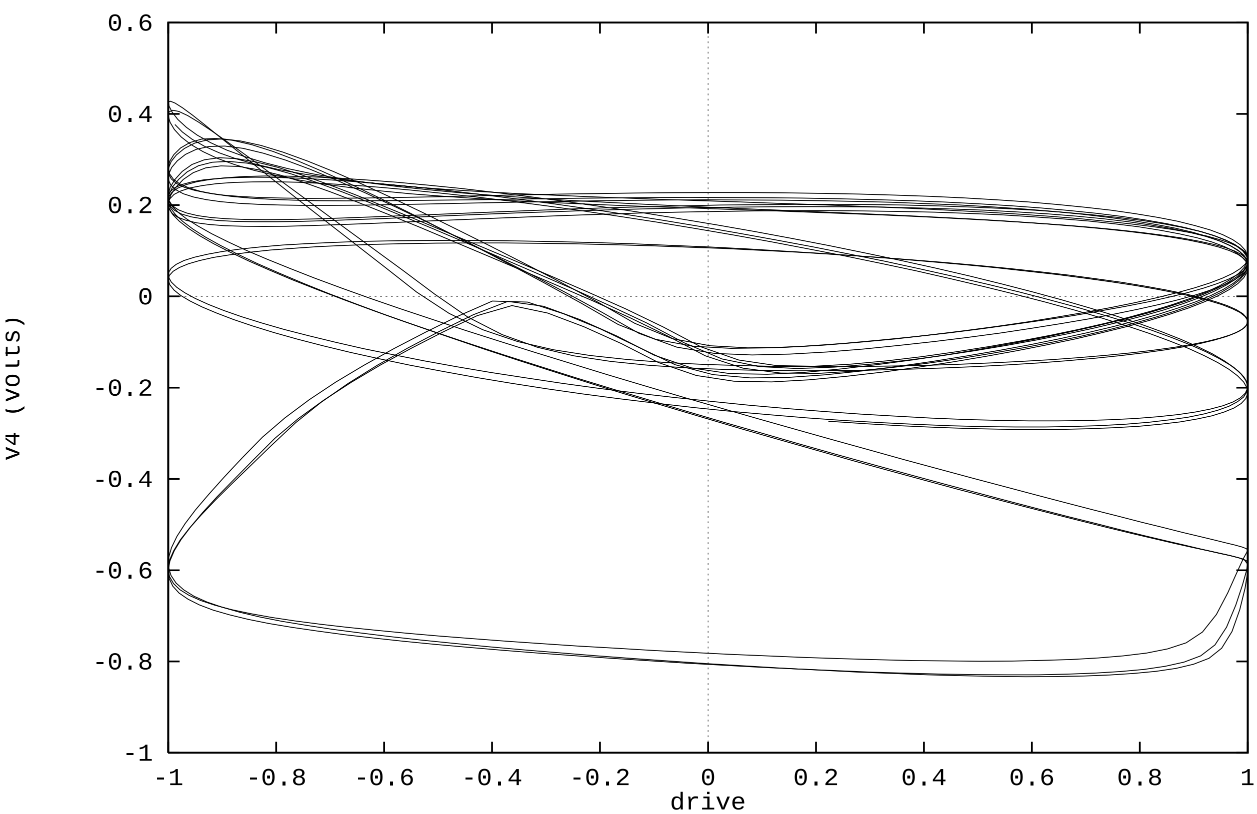

Figure 7. 6-cycle driven oscillator

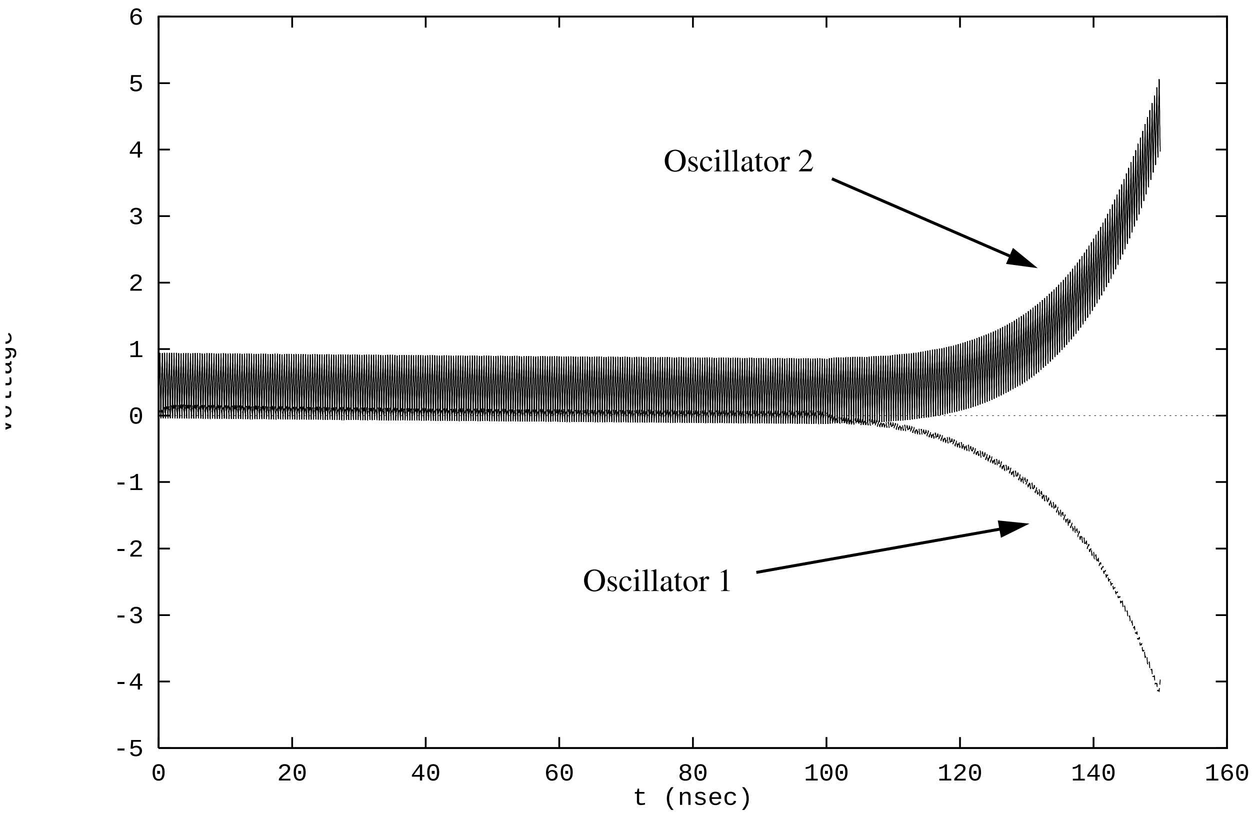

Figure 8. Diverging oscillations

voltage used for the coupling through the transformer winds up with a positive DC offset due to the long time constants of the elements modelling the antenna. This offset gets added directly to the derivative of u_4, which causes it to get large and escapes the ranges where the circuit models are physically valid, as seen in Figure. 8.

In a real system, behavior such as this would be better filtered out by the antenna, which is generally more narrow-band than my circuit model, so that DC and low-frequency components would not couple at all to the other circuit. Some of the elements left out in this model in order to reduce the order of the problem would also start to become significant and keep the voltages constrained. In addition, in a real circuit the initial conditions are generally applied extremely slowly compared to the time scale of the circuit, and there are no problems waiting for the longer transients to dissipate, since that still would generally be less than a millisecond. In a numerical solution, however, a millisecond is about 10^{10} time-steps, which is a prohibitive amount of computational time

It does not appear that corrections to this problem will be easy to implement. Techniques such as subtracting running averages from the voltages across the mutual inductor are able to sta-

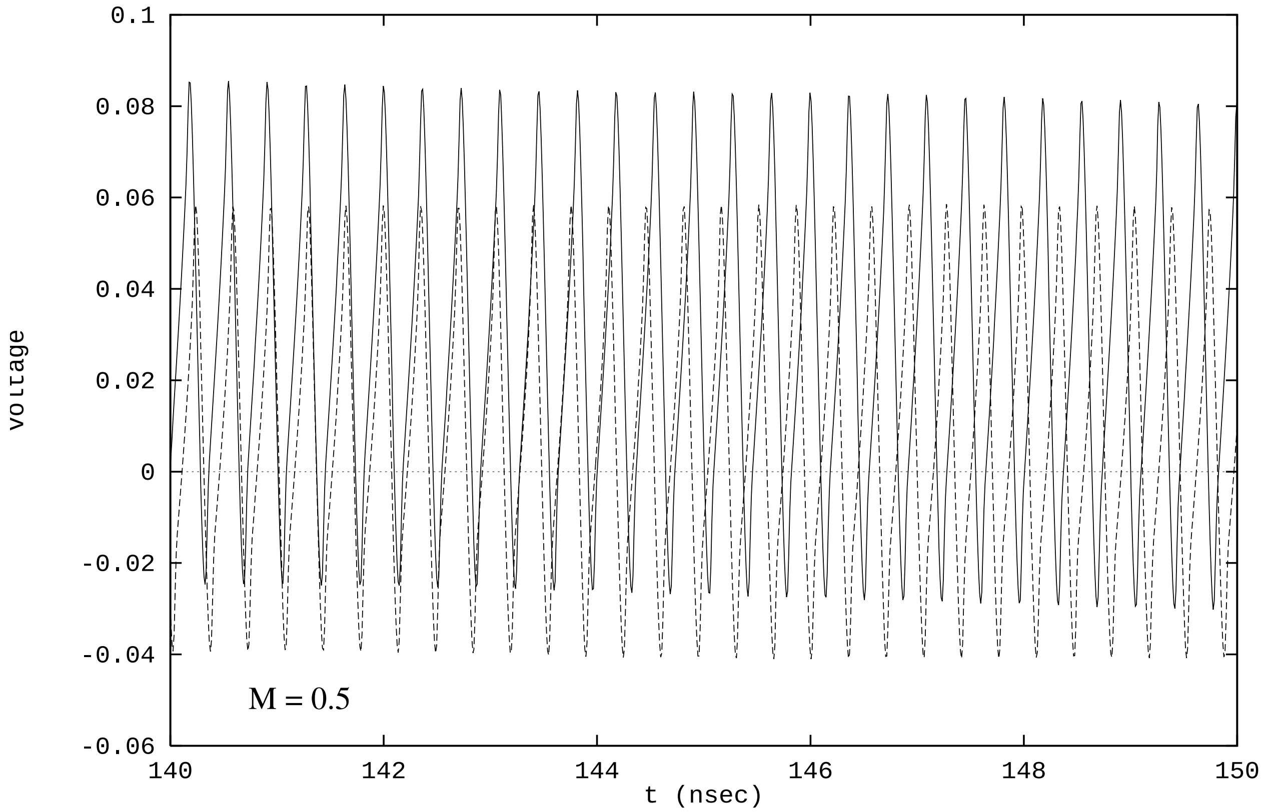

Figure 9. Coupled oscillators - stabilized

bilize the oscillations, as we see in Figure 9. Unfortunately, this stabilization seems to have removed the ability of the two oscillators to lock. A wide variety of values have been tried for M, ranging from 1.5 to -0.5, but no locking is seen when the inductances have had the running average subtracted from them.

VIII. Conclusions

We have seen that it a mathematical model of a microwave FET can be created from circuit theory by using linear circuit elements and a nonlinear FET model. The common-gate configuration seems to work best for the purposes of simulation, and it allows the frequency to be tuned by adjusting the inductance between gate and ground.

This oscillator can then be coupled to a master oscillator, providing a master-slave or injection-locked configuration. We then see that for differing drive frequencies, the ranges of M which provide locking can vary dramatically. More importantly, a result at a lower frequency suggests the presence of chaotic states within the system. This confirms that careful study of the whole system could be useful in designing circuits containing coupled oscillators, since it could indicate which regions in parameter space are more likely to be ill-behaved. This could help the researcher know which areas in parameter space to avoid in their design and recognize what sorts of results in the laboratory indicate that they are approaching regions of chaotic behavior for the circuit.

Unfortunately, results were not obtained for the two-oscillator case due to problems with the behavior of the numeric model for the coupled antenna. These results would be much more useful in interpreting the behavior of a general set of coupled oscillators, since they are a step closer to what a full system would look like.

IX. Future Work

The first thing that needs to be done is to refine the circuit model, especially the representation of the antenna, to correct the problems which arose in the final part of this work. Additional circuit elements may need to be added to get a better representation of the physical structure, especially concentrating on suppressing DC and low-frequency components from being coupled between the oscillators. There are several ways to do this, but they generally will involve adding at least another node to the system, along with two additional first-order ordinary differential equations per node.

Once the numerical problems are corrected, the next step in this is to qualitatively confirm the results experimentally. The first thing that could be tested is the driven oscillator. Using a synthesizer, we can injection-lock the oscillator while having it looking into a simple 50 Ω load. The drive level could then take the place of the coupling coefficient, and then sweeping the synthesizer across a frequency range should allow us to obtain results similar to those found in Figure 6.

Next the coupled oscillator pairs could be examined. Differences in parameter values can be obtained by making a number of different oscillator circuits using the same type of transistor, and the coupling can be changed in a number of ways depending upon how the antenna is implemented. The difficulty in comparing these results directly to the simulations is that absolute numbers for the model parameters and the coupling are fairly difficult to determine.

Once this methodology is verified for a pair of oscillators, the next step is to extend it to larger systems of oscillators. Since there are seven differential equations per oscillator in the current model, this could result in very large systems of equations which would need to be solved. It may become necessary to find ways to reduce the order of the model in order to allow structures like three-dimensional grid geometries [14] to be simulated in a reasonable amount of time.

X. References:

[1] Pozar, D.M., *Microwave Engineering*, Addison-Wesley, Reading, MA, 1990, p.651-658.

[2] Popovic, Z.B., Weikle, R.M. II, Kim, M., and Rutledge, D.B., "A 100-MESFET planar grid oscillator," *IEEE Trans. Microwave Theory Tech.*, vol. MTT-39, p. 193-200.

[3] Hogg, T., and Huberman, B.A., "Generic behavior of coupled oscillators," *Phys Rev A*, vol. 29, no. 1, p. 275-281.

[4] Saito, T., "On a Coupled Relaxation Oscillator," *IEEE Trans Circuits Systems*, vol. CAS-35, p.1149-1155.

[5] Linsay, P.S., and Brailove, A., "Experiments with Coupled Nonlinear Oscillators," *First Experimental Chaos Conference*, World Scientific, 1991, p. 315-326.

[6] D'Humieres, D., Beasley, M.R., Huberman, B.A., and Libchaber, A., "Chaotic states and routes to chaos in the forced pendulum," *Phys Rev A*, vol. 26, no. 6, p. 3483-3496.

[7] Tomita, K., "Periodically forced nonlinear oscillators," *Chaos* (Holden, ed), Princeton, chapter 10.

[8] *HP85150B Microwave and RF Design Systems Component Catalog; Volume 4—Microwave Library Components (Lumped, Ideal, and Nonlinear)*, Hewlett-Packard, Santa Rosa, CA, 1992, chapter 18.

[9] Curtice, W.R., and Ettenberg, M., "A Nonlinear GaAs FET Model for Use in the Design of Output Circuits for Power Amplifiers," *IEEE Trans Microwave Theory Tech.*, vol MTT-33, p. 1383-1394.

[10] Martinex, R.D., and Compton, R.C., "High-Efficiency FET/Microstrip-Patch Oscillators," *IEEE Anten and Prop Mag*, vol. 36, no.1, p. 16-19.

[11] Liao, P., and York, R.A., "A Six-Element Beam-Scanning Array," *IEEE Microwave and Guided Wave Lett.*, vol. 4, p. 20-22.

[12] Ott, E., *Chaos in Dynamical Systems*, Cambridge University Press, New York, NY, 1993, p. 49-51.

[13] Li, T.Y., and Yorke, J.A., "Period Three Implies Chaos," *Am. Math. Monthly*, vol. 82, p. 985.

[14] Shiroma, W.A., Shaw, B.L, and Popovic, Z.B., "Three-Dimensional Power Combiners," to appear in *1994 IEEE MTT Symposium Digest*.